US009012102B2

(12) **United States Patent**
Han et al.

(10) **Patent No.: US 9,012,102 B2**
(45) **Date of Patent: Apr. 21, 2015**

(54) **PROCESS TO RECOVER PERFORMANCE OF FUEL CELL CATALYSTS**

(75) Inventors: **Taehee Han**, Farmington Hills, MI (US); **Nilesh Dale**, Farmington Hills, MI (US); **Kevork Adjemian**, Birmingham, MI (US)

(73) Assignee: **Nissan North America, Inc.**, Franklin, TN (US)

(*) Notice: Subject to any disclaimer, the term of this patent is extended or adjusted under 35 U.S.C. 154(b) by 291 days.

(21) Appl. No.: **13/210,739**

(22) Filed: **Aug. 16, 2011**

(65) **Prior Publication Data**

US 2013/0045430 A1 Feb. 21, 2013

(51) **Int. Cl.**
H01M 8/04 (2006.01)
H01M 8/10 (2006.01)

(52) **U.S. Cl.**
CPC .. ***H01M 8/04223*** (2013.01); *H01M 2008/1095* (2013.01); *H01M 2250/20* (2013.01); *Y02E 60/50* (2013.01); *Y02T 90/32* (2013.01)

(58) **Field of Classification Search**
None
See application file for complete search history.

(56) **References Cited**

U.S. PATENT DOCUMENTS

2003/0152816	A1	8/2003	Hoch	
2010/0035098	A1	2/2010	Ramani et al.	
2010/0173212	A1*	7/2010	Senoue et al.	429/432
2010/0203407	A1	8/2010	Iden et al.	
2010/0227756	A1*	9/2010	Kim et al.	502/101
2011/0008686	A1	1/2011	Gould et al.	

FOREIGN PATENT DOCUMENTS

JP	2010-027298		2/2010
JP	2010027298	A *	2/2010
WO	2007088471	A1	8/2007

OTHER PUBLICATIONS

Gould et al.,Operational performance recovery of SO2-contaminated proton exchange membrane fuel cells, J. Electrochem. Soc.,2010, 157, B1569-B1577.*

Kothandaraman, Non-precious oxygen reduction catalysts prepared by high-pressure pyrolysis for low-temperature fuel cells, Appl. Catal. B: environmental, 2009, 209-216.*

Shao, Y., Nitrogen-doped carbon nanostructures and their composites as catalytic materials for proton exchange membrane fuel cell, Oct. 12, 2007, Applied Catalysis B: Environmental, 79, 89-99.*

(Continued)

Primary Examiner — Ula C Ruddock
Assistant Examiner — Daniel Gatewood
(74) *Attorney, Agent, or Firm* — Young Basile Hanlon & MacFarlane, P.C.

(57) **ABSTRACT**

Disclosed herein are processes for recovering performance of fuel cells by recovering fuel cell catalyst activity and methods of testing the durability and activity performance of fuel cells. One catalyst recovery process disclosed herein for a fuel cell having a membrane electrode assembly comprises operating the fuel cell for a first recovery cycle with fuel gas supplied to an anode of the fuel cell and an oxidant supplied to a cathode of the fuel cell while drawing a current from the fuel cell at steady state throughout the first recovery cycle, the first recovery cycle having a predetermined time period. The fuel cell has reached end of life due in part to intermittent use prior to operating the fuel cell for the first recovery cycle. A life of the fuel cell improves when the first recovery cycle is complete.

20 Claims, 11 Drawing Sheets

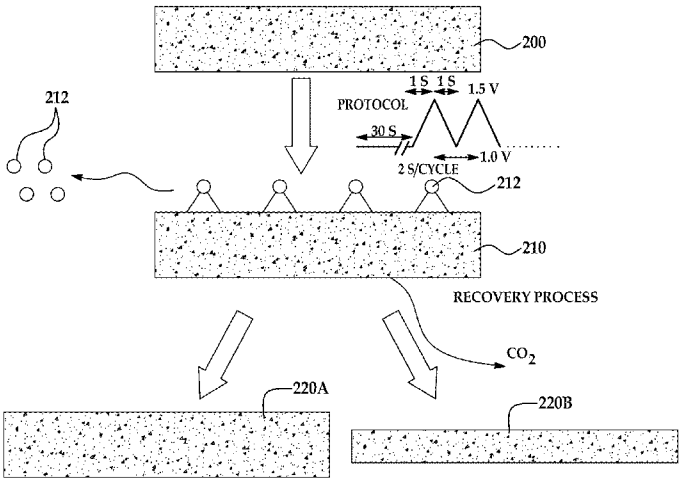

(56) **References Cited**

OTHER PUBLICATIONS

Takeuchi, Norimitsu; Fuller, Thomas F., "Modeling and Investigation of Design Factors and Their Impact on Carbon Corrosion of PEMFC Electrodes", Journal of the Electrochemical Society, 155 (7) B770-B775 (2008) (6 pp).

Urdampilleta, Idoia G.; Uribe, Francisco A.; Rockward, Tommy; Brosha, Eric L.; Pivovar, Bryan S.; Garzon, Fernando H.; "PEMFC Poisoning With H2S: Dependence on Operating Conditions", ECS Transactions, 11 (1) 831-842 (2007) (12 pp).

Shao et al. Nitrogen-doped carbon nanostructures and their composites as catalytic materials for proton exchange membrane fuel cell. Applied Catalysis B: Environmental, vol. 79, 2008, pp. 89-99 [online], [retrieved Aug. 29, 2013]. Retrieved from the Internet <URL:http://www.sciencedirect.com/science/article/pii/S0926337307003293>.

* cited by examiner

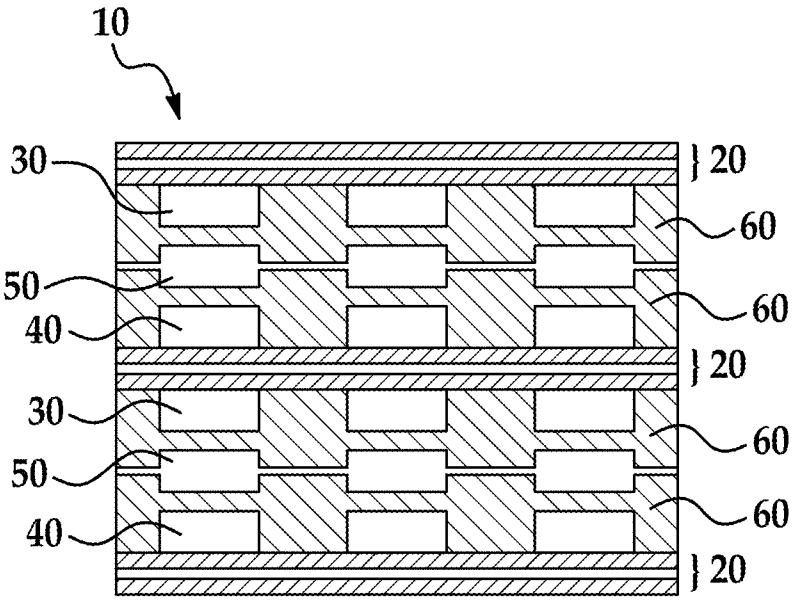
10
30
20
60
50
60
40
20
30
60
50
60
40
20

FIG. 1

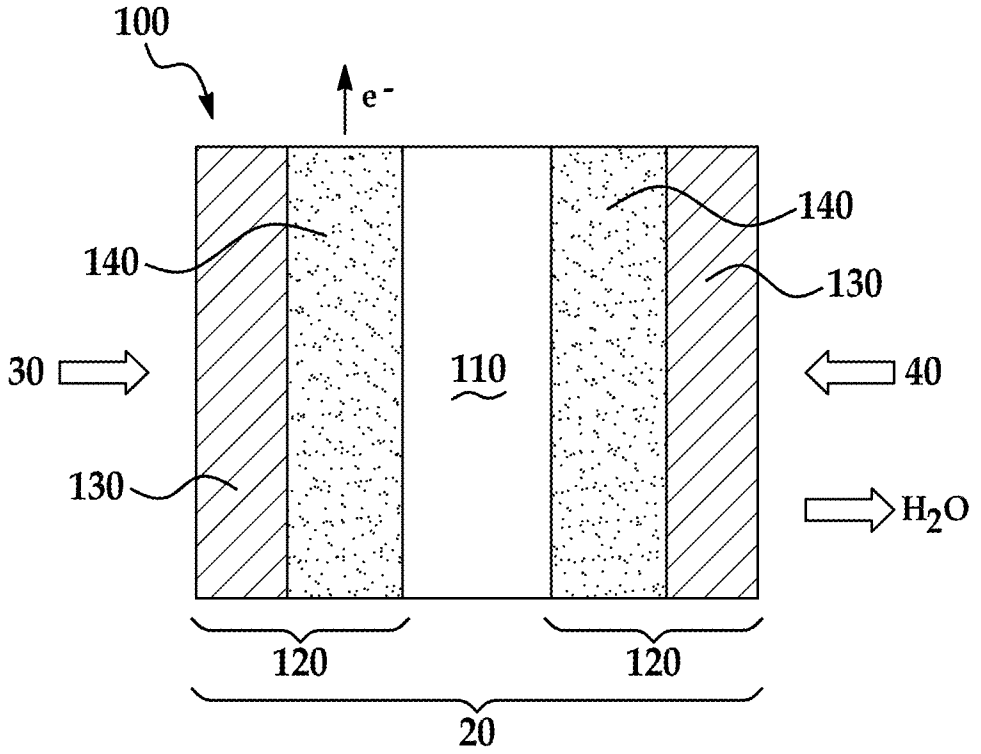
100
e-
140
140
130
30
110
40
130
H2O
120
120
20

FIG. 2

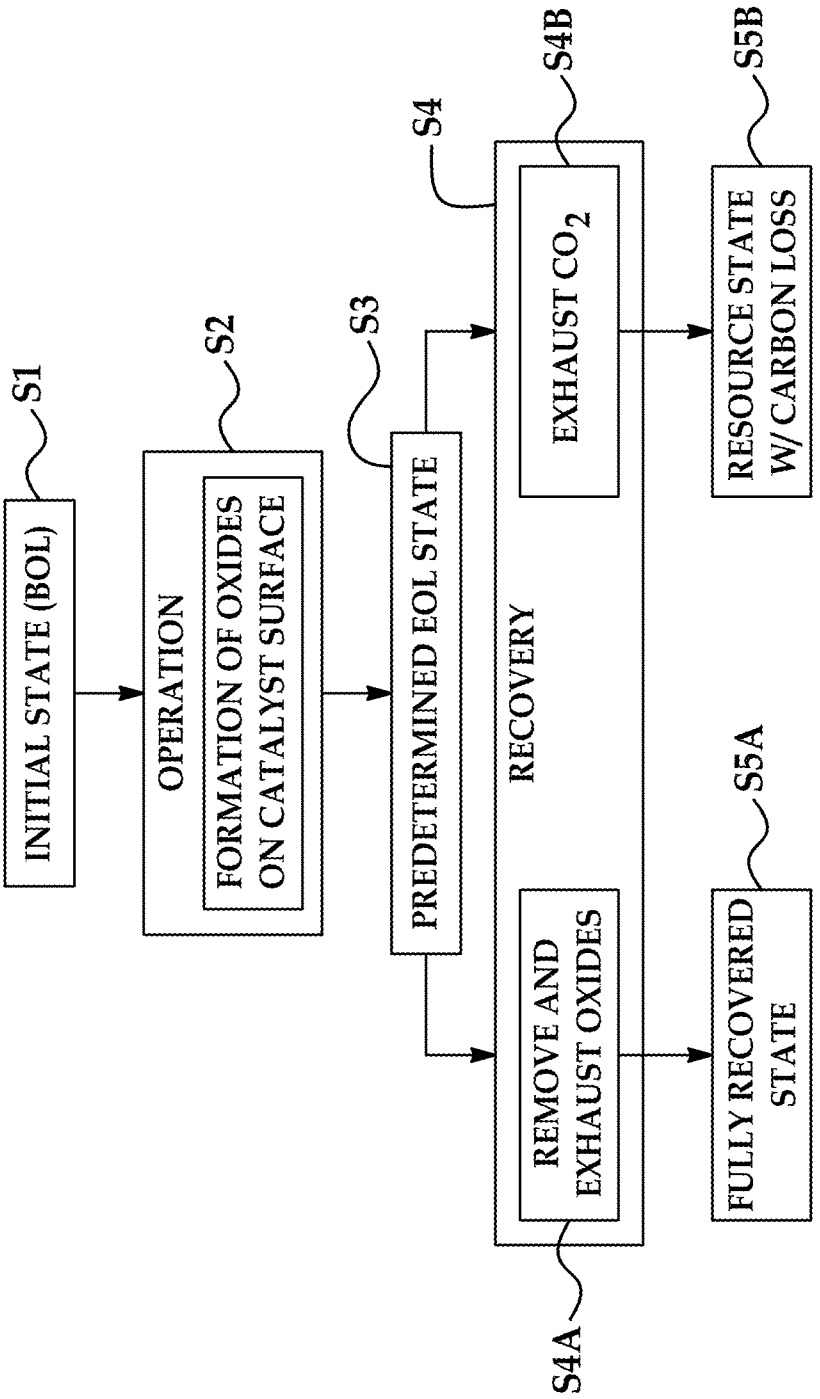
INITIAL STATE (BOL)
S1
OPERATION
FORMATION OF OXIDES ON CATALYST SURFACE
S2
PREDETERMINED EOL STATE
S3
RECOVERY
S4
EXHAUST CO_2
S4B
RESOURCE STATE W/ CARBON LOSS
S5B
REMOVE AND EXHAUST OXIDES
S4A
FULLY RECOVERED STATE
S5A

FIG. 3

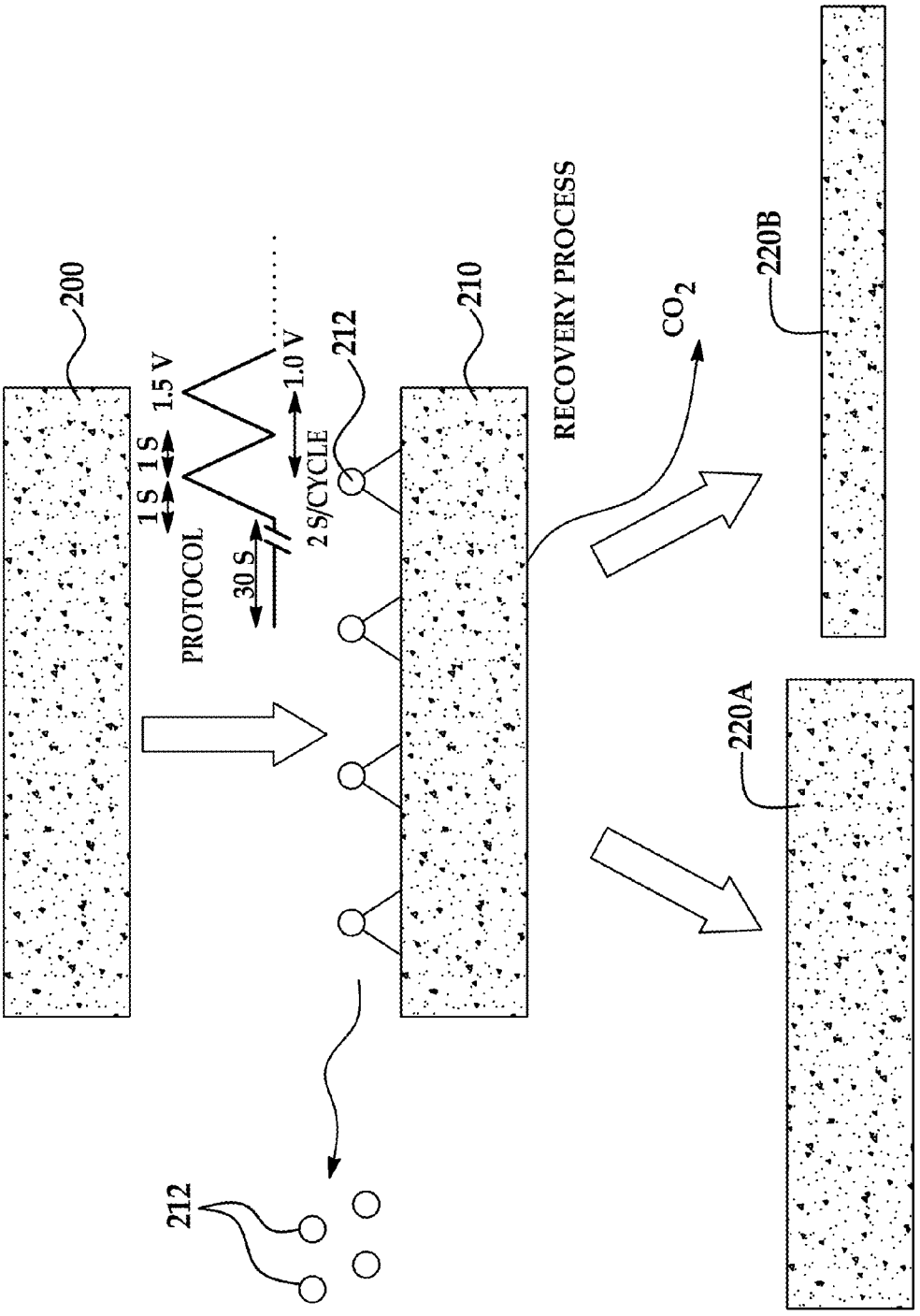
200
1.5 V
1 S 1 S
PROTOCOL
30 S
1.0 V
2 S/CYCLE
212
210
RECOVERY PROCESS
CO_2
220B
220A
212

FIG. 4

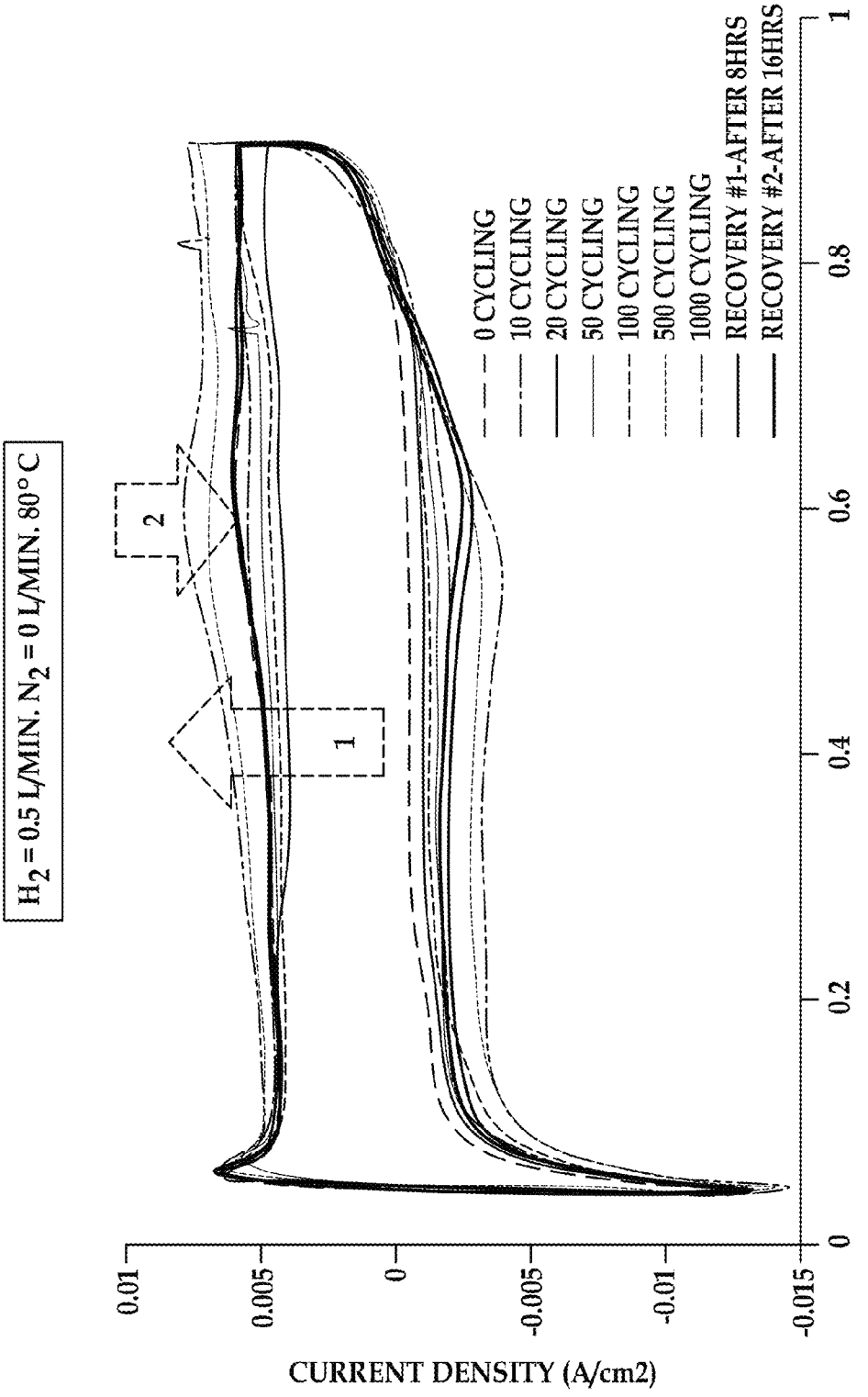
H_2 = 0.5 L/MIN. N_2 = 0 L/MIN. 80° C
1
2
0 CYCLING
10 CYCLING
20 CYCLING
50 CYCLING
100 CYCLING
500 CYCLING
1000 CYCLING
RECOVERY #1-AFTER 8HRS
RECOVERY #2-AFTER 16HRS
0.01
0.005
0
-0.005
-0.01
-0.015
0
0.2
0.4
0.6
0.8
1
CURRENT DENSITY (A/cm2)
POTENTIAL (V)

FIG. 5

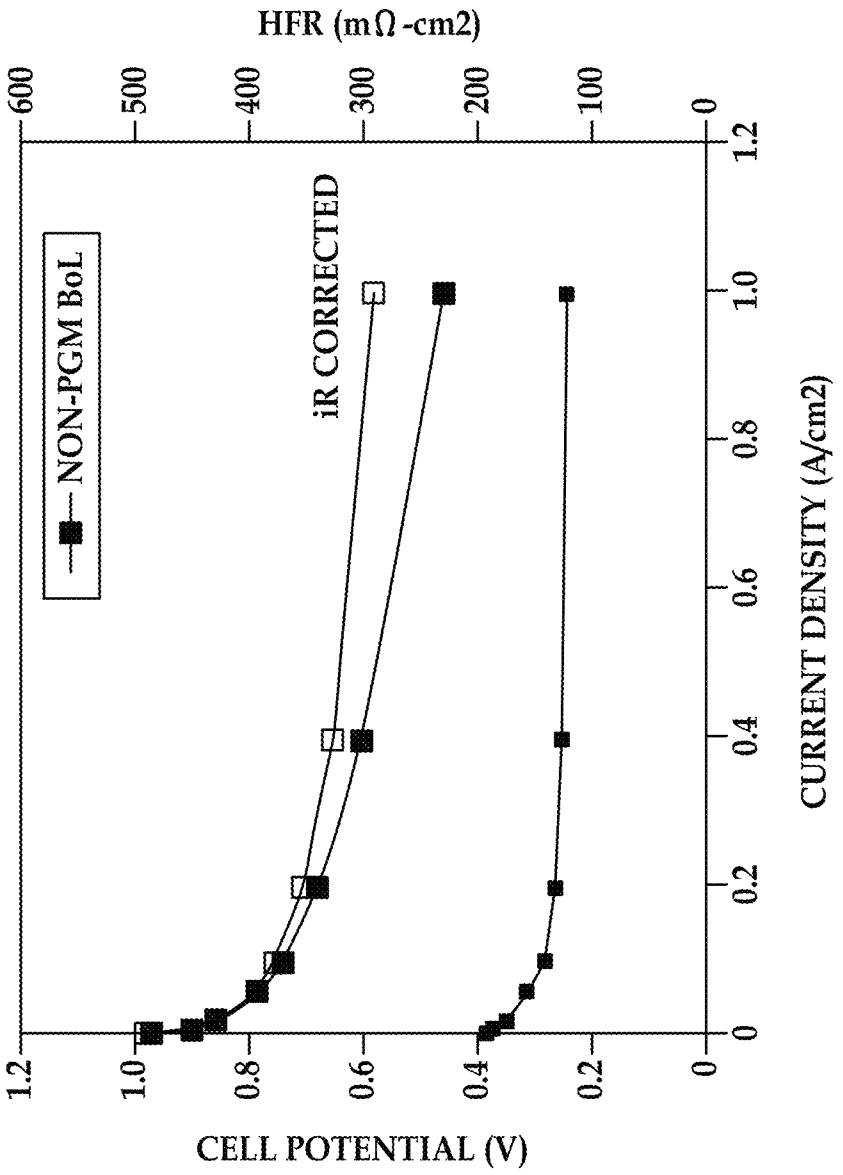
HFR (mΩ-cm2)
600
500
400
300
200
100
0
NON-PGM BoL
iR CORRECTED
1.2
1.0
0.8
0.6
0.4
0.2
0
CELL POTENTIAL (V)
1.2
1.0
0.8
0.6
0.4
0.2
0
CURRENT DENSITY (A/cm2)

FIG. 6A

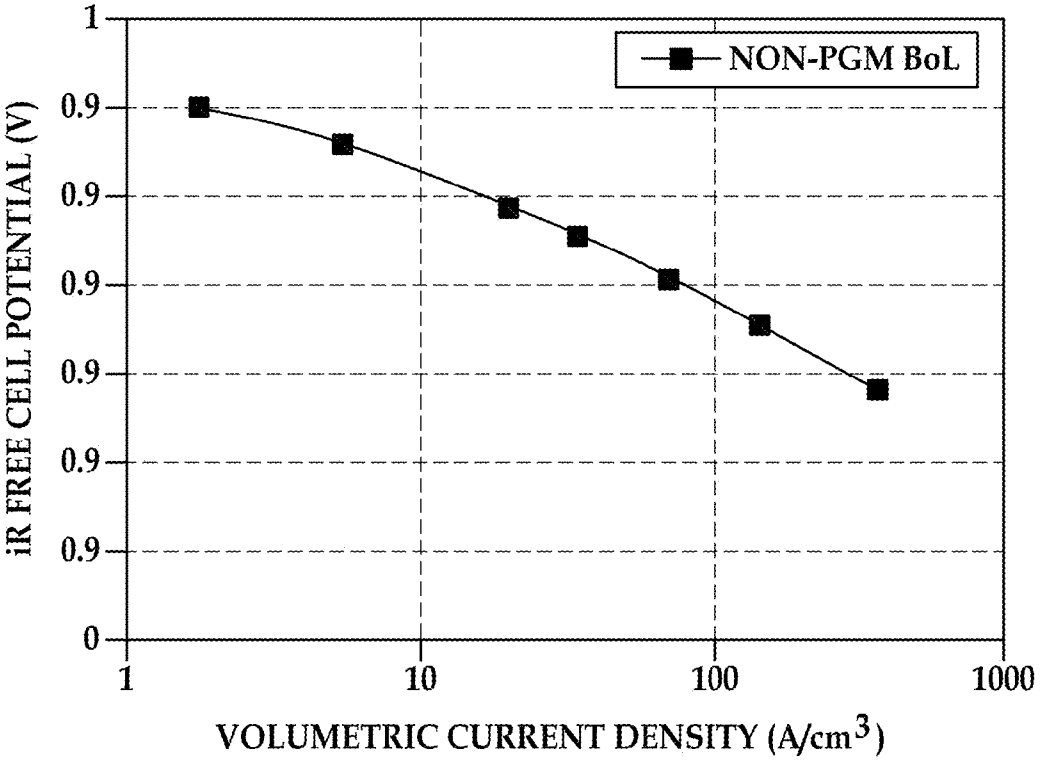
NON-PGM BoL
iR FREE CELL POTENTIAL (V)
1
0.9
0.9
0.9
0.9
0.9
0.9
0
1
10
100
1000
VOLUMETRIC CURRENT DENSITY (A/cm3)

FIG. 6B

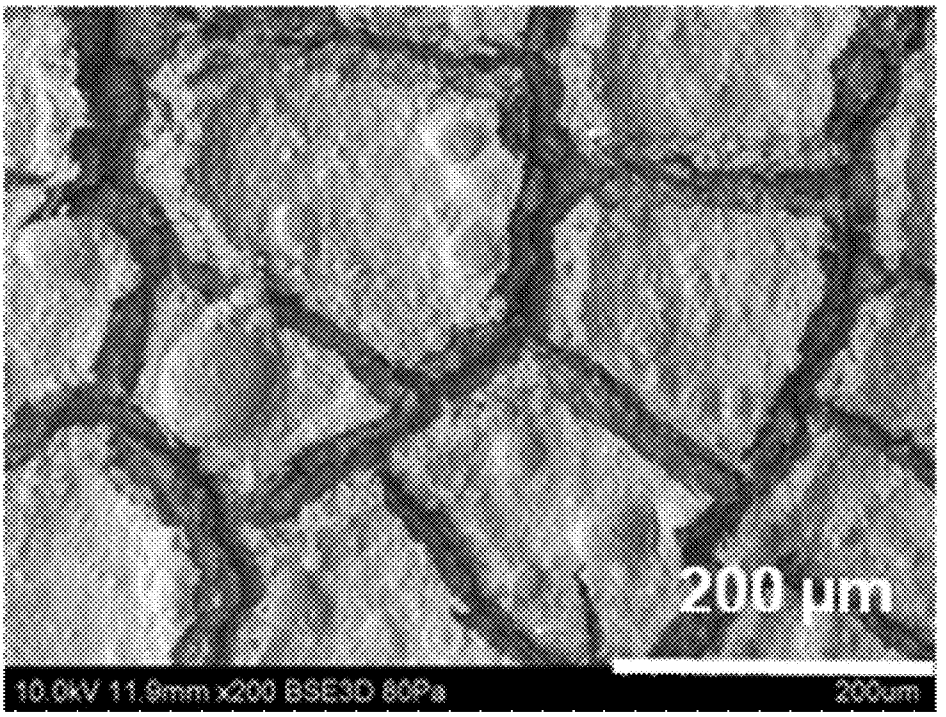
200 µm

FIG. 7A

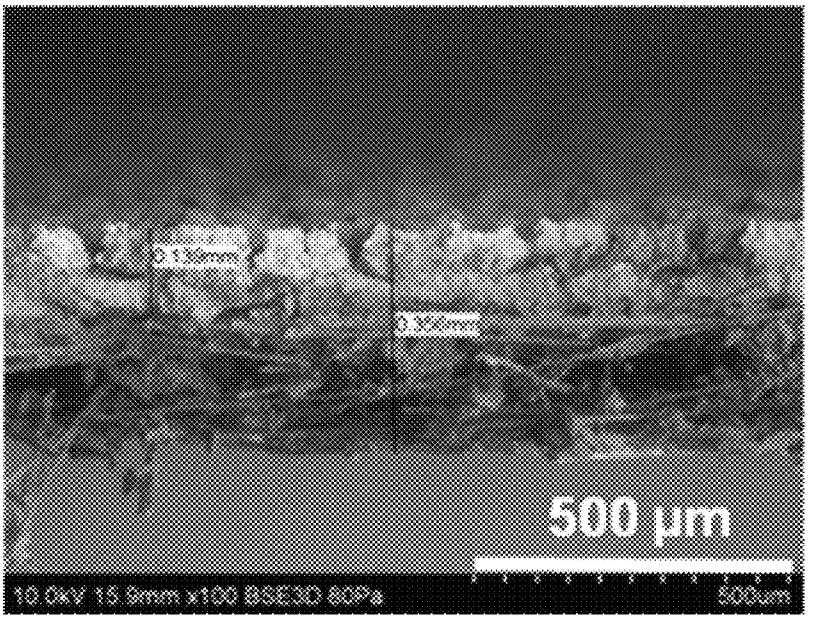
500 µm

FIG. 7B

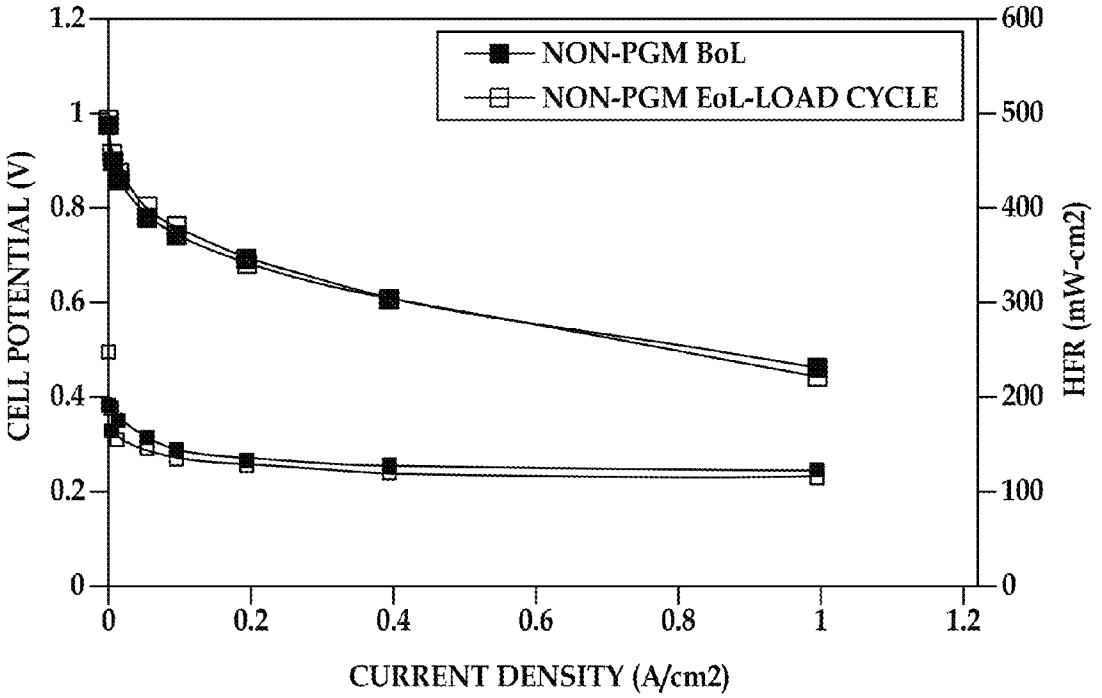
NON-PGM BoL
NON-PGM EoL-LOAD CYCLE
CELL POTENTIAL (V)
HFR (mW-cm2)
CURRENT DENSITY (A/cm2)
0
0.2
0.4
0.6
0.8
1
1.2
0
100
200
300
400
500
600

FIG. 8A

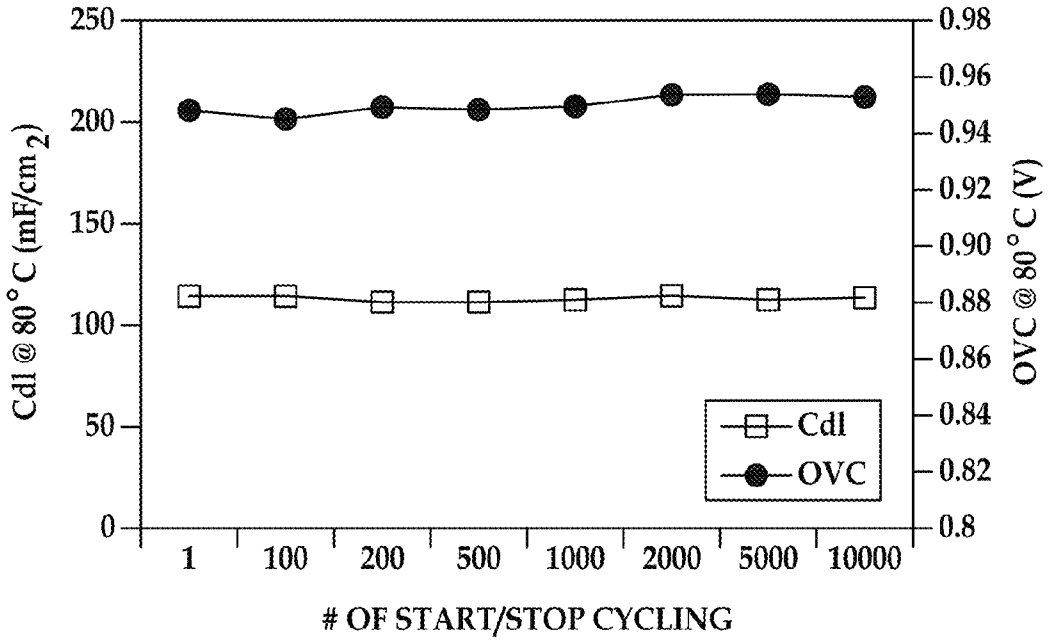
250
200
150
100
50
0
0.98
0.96
0.94
0.92
0.90
0.88
0.86
0.84
0.82
0.8
Cdl @ 80° C (mF/cm 2)
OVC @ 80° C (V)
Cdl
OVC
1
100
200
500
1000
2000
5000
10000
OF START/STOP CYCLING

FIG. 8B

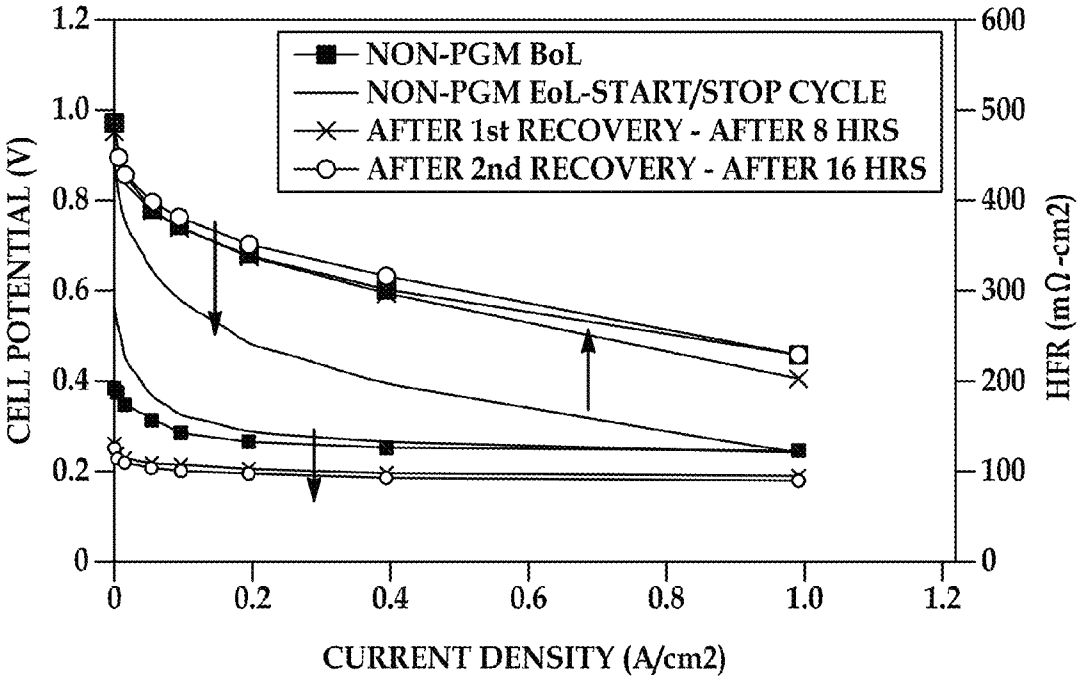
1.2
1.0
0.8
0.6
0.4
0.2
0
600
500
400
300
200
100
0
CELL POTENTIAL (V)
HFR (mΩ-cm2)
NON-PGM BoL
NON-PGM EoL-START/STOP CYCLE
AFTER 1st RECOVERY - AFTER 8 HRS
AFTER 2nd RECOVERY - AFTER 16 HRS
0
0.2
0.4
0.6
0.8
1.0
1.2
CURRENT DENSITY (A/cm2)

FIG. 9A

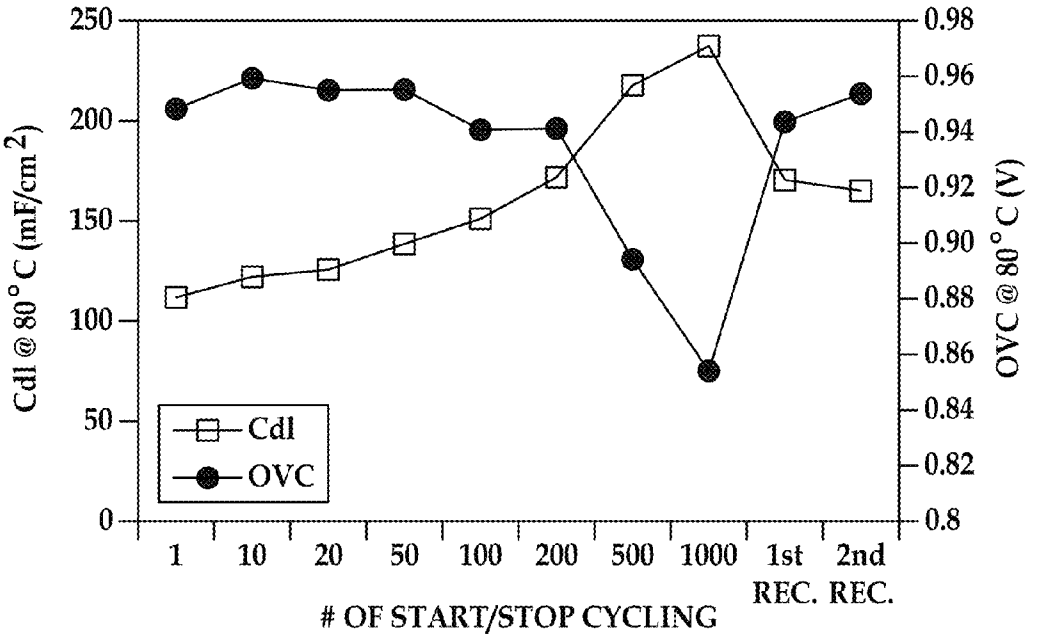
250
200
150
100
50
0
Cdl @ 80 °C (mF/cm 2)
0.98
0.96
0.94
0.92
0.90
0.88
0.86
0.84
0.82
0.8
OVC @ 80 °C (V)
Cdl
OVC
1
10
20
50
100
200
500
1000
1st REC.
2nd REC.
OF START/STOP CYCLING

FIG. 9B

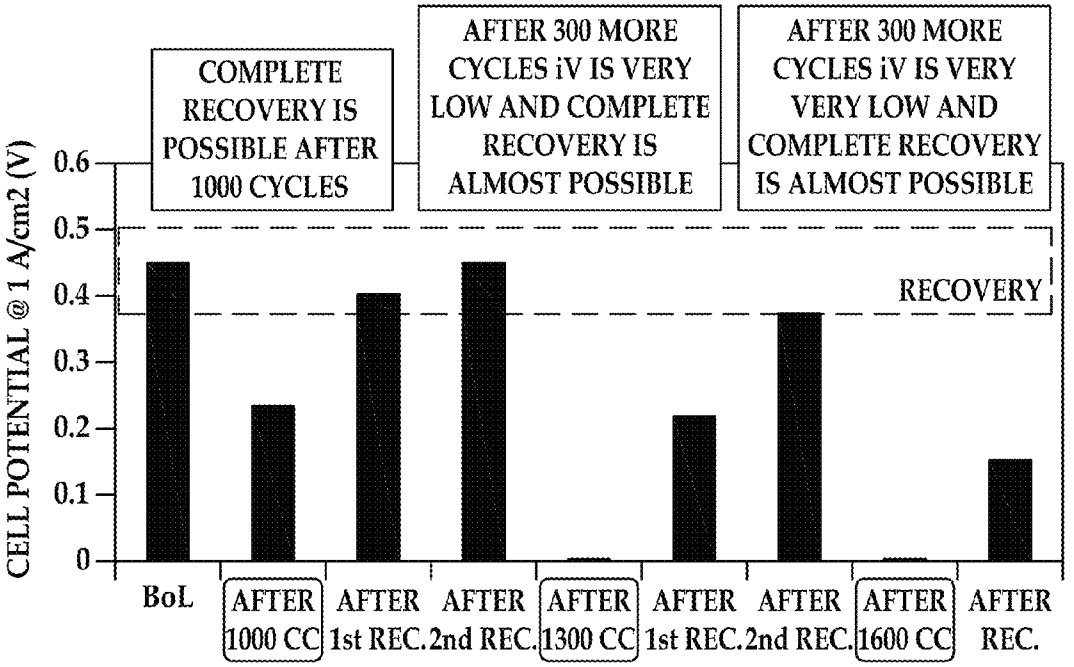
COMPLETE RECOVERY IS POSSIBLE AFTER 1000 CYCLES
AFTER 300 MORE CYCLES iV IS VERY LOW AND COMPLETE RECOVERY IS ALMOST POSSIBLE
AFTER 300 MORE CYCLES iV IS VERY VERY LOW AND COMPLETE RECOVERY IS ALMOST POSSIBLE
RECOVERY
CELL POTENTIAL @ 1 A/cm2 (V)
0.6
0.5
0.4
0.3
0.2
0.1
0
BoL
AFTER 1000 CC
AFTER 1st REC.
AFTER 2nd REC.
AFTER 1300 CC
AFTER 1st REC.
AFTER 2nd REC.
AFTER 1600 CC
AFTER REC.

FIG. 10

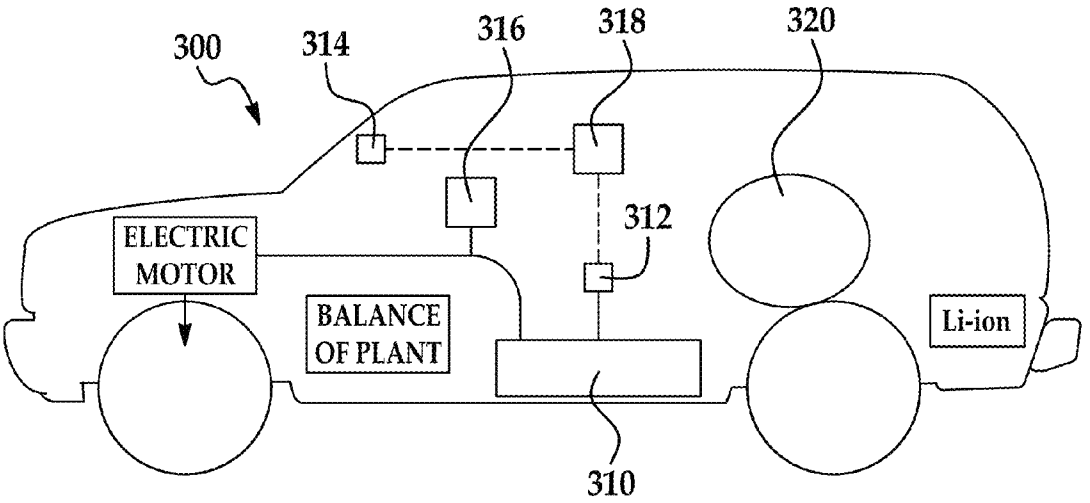
300
314
316
318
320
312
ELECTRIC MOTOR
BALANCE OF PLANT
Li-ion
310

FIG. 11

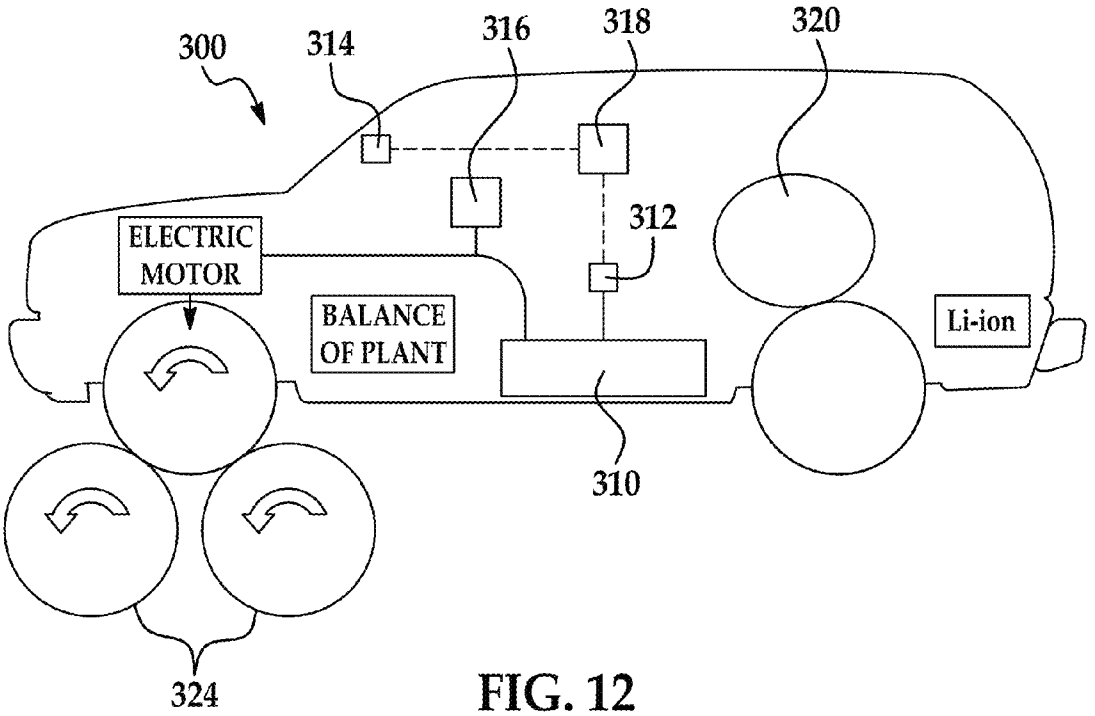
300
314
316
318
320
312
ELECTRIC MOTOR
BALANCE OF PLANT
Li-ion
310
324

FIG. 12

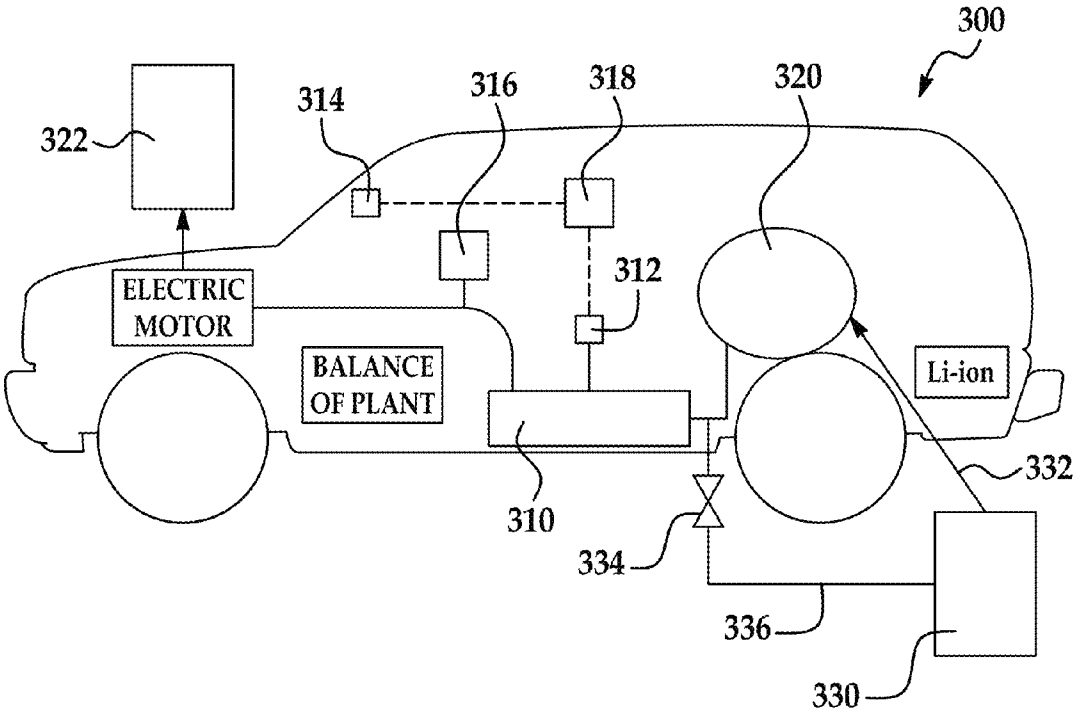
300
322
314
316
318
320
312
ELECTRIC MOTOR
BALANCE OF PLANT
Li-ion
332
310
334
336
330

FIG. 13

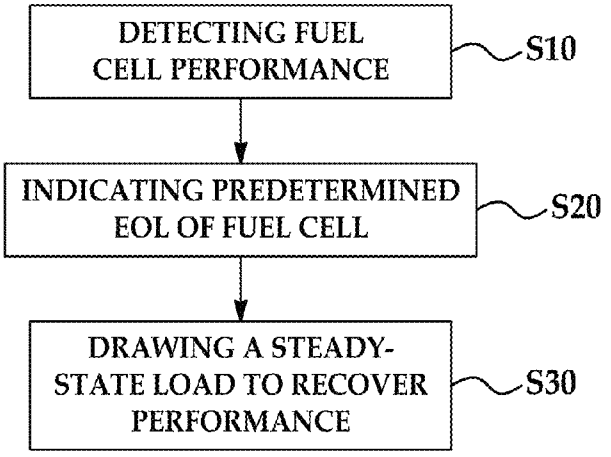
DETECTING FUEL CELL PERFORMANCE
S10
INDICATING PREDETERMINED EOL OF FUEL CELL
S20
DRAWING A STEADY-STATE LOAD TO RECOVER PERFORMANCE
S30

FIG. 14

PROCESS TO RECOVER PERFORMANCE OF FUEL CELL CATALYSTS

BACKGROUND

Platinum and other precious metal-based catalysts have proven to provide superior performance to proton exchange membrane fuel cell technology. One of the major hurdles for mass-commercialization of proton exchange membrane fuel cell vehicles is their high cost. This is due, in particular, to the usage of platinum and other precious group metals as the electrocatalyst. Two potential strategies to reduce the cost are to either significantly lower the loading of platinum/precious group metals (PGM) or by using non-precious group metal (non-PGM) catalysts such as metal-nitrogen-carbon (MNC) type catalysts. So far, however, performance of non-PGM based electrocatalysts for the oxygen reduction reaction (ORR) in polymer electrolyte membrane fuel cells has been no match against the performance of PGM based catalysts, in part because they have a relatively low number of active sites per unit volume.

SUMMARY

Disclosed herein are processes for recovering performance of fuel cells by recovering fuel cell catalyst activity and methods of testing the durability and activity performance of fuel cells. The catalyst recovery process disclosed herein for a fuel cell having a membrane electrode assembly comprises operating the fuel cell for a first recovery cycle with fuel gas supplied to an anode of the fuel cell and an oxidant supplied to a cathode of the fuel cell while drawing a current from the fuel cell at steady state throughout the first recovery cycle, the first recovery cycle having a predetermined time period. The fuel cell has reached end of life due in part to intermittent use prior to operating the fuel cell for the first recovery cycle. A life of the fuel cell improves when the first recovery cycle is complete.

One such recovery process disclosed herein comprises detecting a predetermined end of life state of the fuel cell and performing a first recovery cycle on the fuel cell. The first recovery cycle comprises supplying fuel gas to an anode of the fuel cell and an oxidant to a cathode of the fuel cell and concurrently drawing a current from the fuel cell at steady state for a predetermined time period. The predetermined time period is determined based on near or complete recovery of the fuel cell to an initial state of the fuel cell, with the initial state being a state of the fuel cell prior to operating the fuel cell.

One method of testing durability of catalyst for use in a fuel cell having a membrane electrode assembly comprises performing start/stop cycling on a fuel cell at beginning of life until the fuel cell reaches a predetermined end of life state, supplying fuel gas to an anode of the fuel cell and an oxidant to a cathode of the fuel cell under steady state conditions for a predetermined period of time while drawing a current from the fuel cell, wherein the supplying improves the life of the fuel cell and testing the fuel cell to determine an amount of improvement in performance after the predetermined period of time lapses.

BRIEF DESCRIPTION OF THE DRAWINGS

The various features, advantages and other uses of the present apparatus will become more apparent by referring to the following detailed description and drawing in which:

FIG. **1** is a schematic cross-sectional illustration of a basic fuel cell stack having multiple fuel cells;

FIG. **2** is an enlarged schematic cross-sectional view of a membrane electrode assembly from the fuel cell stack of FIG. **1**;

FIG. **3** is a flow diagram of the recovery process;

FIG. **4** is a schematic of the recovery process;

FIG. **5** is a fuel cell cyclic voltammetry plot before and after carbon corrosion and the recovery process;

FIG. **6**A is a graph showing BOL iV performance measured at one bar pressure with and without iR correction data;

FIG. **6**B is a graph showing volumetric activity or volumetric current density;

FIG. **7**A is an SEM image of a metal-nitrogen-carbon catalyst based GDE showing surface morphology at 200×;

FIG. **7**B is an SEM cryofractured cross-sectional view of the metal-nitrogen-carbon catalyst based GDE at 100×;

FIG. **8**A is a graph showing the effect of load cycling only on iV performance (H_2/O_2 fully humidified at 80° C. and 100 kPa_g);

FIG. **8**B is a graph showing the double layer capacitance (C_{dl}) or OCV (H_2/O_2 0.5 nlpm for both anode and cathode under atmospheric pressure) values;

FIG. **9**A is a graph showing the effect of start-stop cycling and the recovery processes on iV performance (H_2/O_2 fully humidified at 80° C. and 100 kPa_g);

FIG. **9**B is a graph depicting C_{dl} and OCV values (H_2/O_2 0.5 nlpm for both anode and cathode under atmospheric pressure);

FIG. **10** is a graph showing the effect of the start-stop cycling and the recovery process on the cell potential at 1 A/cm^2;

FIG. **11** is a schematic of a recovery process system;

FIG. **12** is a schematic of another embodiment of a recovery process system;

FIG. **13** is a schematic of another embodiment of a recovery process system; and

FIG. **14** is a flow diagram of a method of operating a recovery process system.

DETAILED DESCRIPTION

FIG. **1** shows a schematic cross-sectional illustration of a portion of a fuel cell stack **10**. The illustration is provided as an example of the fuel cell electrodes and is not meant to be limiting. The fuel cell stack **10** is comprised of multiple membrane electrode assemblies **20**. Fuel **30** such as hydrogen is fed to the anode side of a membrane electrode assembly **20**, while an oxidant **40** such as oxygen or air is fed to the cathode side of the membrane electrode assembly **20**. Coolant **50** is supplied between the fuel **30** and oxidant **40**, the coolant **50** separated from the fuel **30** and oxidant **40** by separators **60**.

Each fuel cell in the fuel cell stack **10** comprises a catalyst. Conventional PGM catalyst used in fuel cells is particles of an electrically conductive material, typically in powder form, which can comprise, for example, carbon as a support structure supporting a metal which is insoluble or only very slightly soluble in water with low oxidation sensitivity. Non-limiting examples of such a metal include titanium, gold, platinum, palladium, silver and nickel and mixtures thereof. The carbon support of the catalyst is electrically conductive and porous, so that sufficient conductivity and gas-permeability of the catalytic layer is ensured. Carbon minimizes electronic resistance of the electrode while the precious metal serves as the catalyst for the electrochemical reaction.

FIG. **2** is exemplary of one of the plurality of fuel cells **100** in the fuel cell stack **10**. The fuel cell **100** can be comprised of

a single membrane electrode assembly **20**. The membrane electrode assembly **20** has an electrolyte membrane **110** with a gas diffusion electrode **120** on opposing sides of the membrane **110**. Each gas diffusion electrode **120** has a gas diffusion layer **130** on which a catalyst layer **140** is formed. When fuel **30**, such as hydrogen gas, is introduced into the fuel cell **100**, the catalyst layer **140** of the gas diffusion electrode **120** splits hydrogen gas molecules into protons and electrons. The protons pass through the membrane **110** to react with the oxidant **40**, such as air, forming water (H_2O). The electrons (e^-), which cannot pass through the membrane **110**, must travel around it, thus creating the source of electrical energy.

To reduce the cost of fuel cells and to decrease environmental impact, much effort is being made to increase the performance and durability of non-PGM catalysts for use in fuel cells such as those described with reference to FIGS. **1** and **2**, and in particular for fuel cells used in vehicles. With regard to performance, or activity, metal-nitrogen-carbon (MNC) type non-PGM catalysts have attracted attention due to their high ORR performance compared to other non-PGM catalysts. The MNC type catalysts are typically synthesized by heating precursors of nitrogen, carbon and metal. The metal can be, for example, iron and cobalt. It is believed that the nature of the catalytic active sites and mechanism of ORR at these sites for these MNC type catalysts strongly depends on the nitrogen and the metal precursor types, heat treatment temperature and carbon support morphology. It has also been demonstrated that increasing the nitrogen/carbon ratio of the nitrogen precursor increases the accessible active site density by reducing the carbon deposition in the pores of carbon support during pyrolysis.

In addition to performance, durability is also a great challenge for the non-PGM catalysts, including those non-PGM catalysts performing under proton exchange membrane fuel cell operating conditions. Load cycling and start-stop cycling are two critical durability tests to identify the stability of a catalyst for proton exchange membrane fuel cells.

Load cycling for a PGM cathode catalyst is typically conducted at a relatively low potential range (0.6-0.95V) to simulate the normal fuel cell operating voltage range. This load cycling results in PGM catalyst degradation due to platinum (or other precious metal group) dissolution and migration. This PGM catalyst degradation can be mainly ascribed to (i) precious metal dissolution and redeposition (Oswald reopening process) and (ii) precious metal agglomeration due to precious metal nanocrystallite migration and/or loss of support. Due to the absence of precious metal groups in the non-PGM catalysts, the effect from the load cycling on the non-PGM catalyst is minimal.

Generally, a fuel cell catalyst's in-situ performance and durability can be evaluated by its iV (current and voltage) characteristics under various operating conditions and potential cycling tests under accelerated operating conditions. One of the important catalyst durability tests is the start-stop (carbon corrosion) test. It evaluates the stability of carbon support for a fuel cell catalyst during potential cycling. This accelerated durability protocol simulates the repeated start-up and shut down of a fuel cell stack in actual operation without the application of any operational controls that may mitigate the losses. This durability protocol can be applied to both PGM and non-PGM fuel cell catalyst having carbon support.

Non-PGM catalyst, however, is more severely deteriorated than PGM catalyst by the start-stop cycling of the fuel cell in which it operates. This is because the majority of the non-PGM catalyst is carbon. This start/stop cycling is particularly prominent when the fuel cell is used to power a vehicle. However, the start/stop cycling can occur in any appliance or device powered by a fuel cell where starting and stopping of the device occurs frequently throughout the life of the fuel cell.

Start/stop cycling can be simulated by simulating in rapid succession load variations including load cessation and bringing load from cessation to an operating load with such frequency to simulate the operating, starting and stopping over a lifetime of use of the fuel cell, such as would be experienced by a fuel cell used in a vehicle, also described as intermittent use. During the start-stop cycling, degradation of the catalyst occurs due to corrosion of the carbon in the catalyst. Surface oxides form on the surface of the carbon, forming a passive layer on the catalyst surface. This surface oxide decreases the performance of the catalyst and therefore the fuel cell. Complete oxidation of carbon is also possible which results in permanent loss of carbon from the non-PGM catalyst.

To compromise for the lower activity per volume of non-PGM catalyst, non-PGM catalyst layers should be around 10 times thicker (~100 μm) than PGM catalyst layers (~10 μm). Therefore, an attempt was made to electrochemically remove the surface oxides formed during the start-stop cycling durability testing to regenerate the catalyst surface with an expectation of partial or full recovery of performance of the non-PGM catalyst.

The recovery process disclosed herein regenerates a catalyst used in fuel cells after the performance has been degraded due to load and/or start-stop cycling. The recovery process can be performed on either PGM or non-PGM catalysts. The disclosure concentrates on non-PGM catalysts due to the increased thickness and therefore a larger amount of carbon.

A fuel cell prior to any use has beginning of life (BOL) characteristics. As used herein, "BOL" means the performance potential of the fuel cell prior to any use. BOL can be measured using one or more characteristics such as voltage and current. BOL can be measured using other characteristics depending on the application of the fuel cell. For example, BOL for a fuel cell that powers a motor vehicle may be measured by length of time of operation or distance traveled, such as 0 hours operated or 0 miles traveled. The recovery process regenerates performance in, for example, the non-PGM MNC type catalyst used in fuel cell membrane electrode assemblies after carbon corrosion cycling, when the fuel cell is at end of life (EOL) or has EOL characteristics. As used herein, "EOL" means the point at which the fuel cell is not producing sufficient power to fully operate the device in which it is located. EOL can be measured using one or more characteristics such as voltage and current, or iV (current-voltage measuring system). EOL can be measured using other characteristics depending on the application of the fuel cell. For example, EOL of a fuel cell that powers a motor vehicle may be measured by length of time of operation or distance traveled. The recovery process regenerates the catalyst, bringing the fuel cell from EOL to at or near its BOL performance characteristics after one completion of the recovery process. The catalyst can be regenerated fully to its BOL performance typically after a first recovery process cycle. It is also possible to regenerate catalyst so that a fuel cell's performance potential is greater than its initial BOL if the recovery process is performed in conjunction with preconditioning of the fuel cell. Fuel cells undergo a preconditioning process prior to installation for use. Performing the preconditioning process after the recovery process can further increase the fuel cell's BOL performance characteristics.

Referring to FIG. **3**, the fuel cell is at an initial state equal to BOL prior to any use (S**1**). During operation of the fuel cell, the catalyst is degraded (S**2**) until it reaches a predetermined

EOL state (S3). After the fuel cell catalyst has been degraded, the recovery process (S4) is performed on the fuel cell by operating the fuel cell at steady state, supplying hydrogen to the anode and the oxidant to the cathode, while a steady current is being drawn from the fuel cell over a predetermined amount of time. The current drawn can be between about 0.3 A/cm^2 to about 0.5 A/cm^2. Higher current than 0.5 A/cm^2 can be drawn from the fuel cell if applicable. The hydrogen and oxidant flow rates can be those used in operation of the fuel cell. For example, the hydrogen flow rate can be about 0.5 nlpm. The hydrogen flow rate can be lower than 0.5 nlpm and the oxidant flow rate can be increased while achieving similar recovery in iV performance. It should be noted that the proper flow rates can vary depending on the geometry of the flow field of the fuel cell.

When referring to regeneration or recovery, it is understood that the catalyst undergoes the electrochemical change while the fuel cell, including the membrane electrode assembly and gas diffusion electrode, or the membrane electrode assembly or gas diffusion electrode alone, recovers performance due to the electrochemical change that the catalyst undergoes during the recovery process.

The pre determined amount of time is based on testing and is the time required to regenerate a predetermined EOL state to at or near the initial state. The initial state before the first recovery is performed is the BOL of the fuel cell prior to use. The initial state for subsequent recovery processes is the state to which the fuel cell is recovered after the previous recovery process. The predetermined amount of time is approximately between 15 to 20 hours. The recovery process can be longer or shorter than the 15 to 20 hour range depending on the type of carbon support and catalyst. As a non-limiting example, graphitized carbon support may require an adjustment in predetermined time. The recovery of PGM catalysts may also require an adjustment in the predetermined time to achieve the desired results. The length of time elapsed between EOL of the fuel cell and the start of the recovery process may affect the predetermined amount of time necessary for the recovery process to achieve the desired results.

The process can be done at ambient pressure. However, the pressure can be higher than ambient pressure, such as 100 kPA_g, thereby reducing the predetermined amount of time necessary to achieve the desired results. For example, performing the process at ambient pressure requires between 15 and 20 hours. Performing the process at a pressure of about 1 to 5 bars can reduce the period necessary to achieve recovery to less than 15 to 20 hours. It should be noted that the pressure will also vary depending on the geometry of the flow field of the fuel cell, which will also affect the necessary time required for recovery.

The oxidant can be oxygen or air, with the use of air resulting in a longer predetermined amount of time necessary to achieve the desired results. Air can be used during the recovery process if the membrane electrode assembly undergoing recovery does not have mass transport limitations and at least 0.3 A/cm^2 current can be drawn from the fuel cell.

This recovery operation causes reactions with the surface oxides on the carbon, allowing the surface oxides to be removed from the surface of the catalyst (S4A) resulting in a fully recovered state (S5A). Carbon dioxide can also be exhausted (S4B), resulting in a fully recovered state with carbon loss (S5B). As mentioned, the resulting condition of the fuel cell can be equal to or near the initial condition of the fuel cell before undergoing the recovery process.

The results of the recovery process may be explained by the electrochemical oxidation processes. During the carbon corrosion durability test, the cell potential is cycled in protocol for the certain number of cycles, for example, 1000 cycles to simulate long term intermittent operation of the device. During this high potential cycling, the carbon surface electrochemically oxidizes to form surface oxides (oxygen containing groups such as carboxyl, carbonyl, phenol, carbonyl etc.) and gaseous carbon dioxide by partial (or incomplete) and complete oxidation pathways, respectively. Generally, at the beginning, incomplete oxidation (formation of surface groups) is dominant over complete oxidation (formation of carbon dioxide, which results in the complete loss of carbon support.) Oxides are generally surface bound so they form a layer on the carbon surface. These surface oxides make the carbon support more hydrophilic so that the catalyst retains more water during fuel cell operation and introduces significant mass transport losses. The passive oxide layer on the catalyst surface also negatively affects the activity of the non-PGM catalyst. The fuel cell iV performance drops significantly due to the formation of these surface oxides as shown in FIG. **9**A.

During this recovery process, the created surface oxides on the catalyst surface are removed. The mechanism for surface oxide removal is one or a combination of the complete oxidization of the surface oxide to carbon dioxide and the reduction of the oxide back to the original catalyst structure. In this process, the electrocatalyst loses some of the carbon support; however, even with some carbon loss, the non-PGM catalyst maintains enough carbon to provide adequate electrochemical activity and electronic conductivity. A schematic of this process is shown in FIG. **4**. The non-PGM catalyst **200** is shown at BOL prior to any use. The non-PGM catalyst **210** is shown with surface oxides **212** after the fuel cell has been in use. The non-PGM catalyst **220**A and B represents non-PGM catalyst **210** after it has undergone the recovery process. As shown, the surface oxides **212** are removed from the carbon in the catalyst **220**A. Some of the carbon of the non-PGM catalyst **210** may form carbon dioxide (CO_2) and be exhausted from the fuel cell during the recovery process, thus reducing the amount of carbon remaining in the non-PGM catalyst **220**B.

Cyclic voltammetry (CV) was performed during the carbon corrosion durability test and before and after the recovery process to verify the formation and removal of surface oxide as shown in FIG. **5**. Formation of surface oxides due to the potential cycling during the carbon corrosion test resulted in increased carbon current and peak appearance at/around 0.6V as shown in FIG. **5**. CV was also measured after each recovery cycle. Reduced carbon current and peak shrinkage at/around 0.6V after each recovery step confirm the removal of surface oxides.

After a certain number of cycles in which the recovery process is performed, depending on the type of carbon support, eventually the electrocatalyst will lose enough carbon that it can not support the required electronic conductivity for fuel cell operation. At this point, the recovery process may no longer recover the iV performance of fuel cell catalyst.

The recovery process disclosed herein when used on non-PGM fuel cell electrocatalyst regenerates catalyst when the fuel cell is at its EOL back to its BOL characteristics, potentially doubling the fuel cell's life. After the recovery process, the recovery in performance is not only observed in the mass transport region but in the kinetic region as well. Subsequent recovery process cycles can be performed on the fuel cell each time the fuel cell reaches the predetermined EOL state. As additional recovery process cycles are performed, the percent recovery of BOL characteristics decreases. The limiting factor of number of recovery process cycles is the amount of

carbon loss, as at a certain amount of carbon loss, the catalyst cannot maintain sufficient electronic conductivity during fuel cell operation.

The recovery process can be done on fuel cells with non-PGM catalyst as a "pre-treatment" prior to first use in operation. It has been seen that the recovery process can actually improve on the BOL characteristics of the fuel cell, thereby enhancing the life cycle of the fuel cell even before it is in use. The recovery process can also be used to partially recover BOL characteristics of fuel cells using PGM catalyst, and in particular, platinum and platinum-alloy catalysts with various types of carbon supports. It is contemplated that the recovery process may be used to remove contamination such as hydrogen sulfide poisoning.

The recovery process is useful in the testing environment as well. The recovery process can be used, for example, to evaluate the durability of the various carbon supports that can be used in both PGM and non-PGM catalysts as further potential cycling can be performed after the recovery process has been done.

To illustrate in detail the recovery process, the following example is provided. A metal-nitrogen-carbon type non-PGM catalyst was produced using a melamine precursor and a high surface area carbon with optimized surface nitrogen content. Ketjenblack 600JD was dispersed in a 95% ethanol solution, to which iron (II) acetate corresponding to 0.75 wt % Fe was added. This slurry was stirred for six hours followed by solvent evaporation to get a dry powder. Powder samples were then ground with pyridinic nitrogen rich precursor melamine (N/C=2.0) to achieve nominal 6.3 wt % N loading. After the post synthesized treatment, the catalyst powder was used to prepare a catalyst ink by mixing with water, ethanol and 20 wt % Nafion solution.

Gas diffusion electrodes (GDEs) with 0.56 mg_{cat}/cm^2 (4 mg_{total}/cm^2) loadings were prepared by spraying the catalyst ink onto a SGL SIGRACET® 25 BCH gas diffusion layer (GDL). Due to the thick catalyst layer, GDEs were pre-pressed at room temperature to avoid any shorting during the hot-pressing due to having a thick and rough catalyst layer surface. Membrane electrode assemblies (MEAs) were prepared by hot-pressing a traditional 0.4 mg_{Pt}/cm^2 loading Pt/C GDE as the anode, a catalyst coated GDE as the cathode and DuPont™ Nafion® NRE211CS as the membrane. Prepared MEAs were evaluated in a 25 cm^2 single cell with serpentine flow fields. Initial conditioning was performed under fully humidified H_2/Air, 0.5 A/cm^2, 80° C. and ambient pressure for 16 hours. After initial conditioning and BOL iV performance measurements, the MEA was subjected to a load cycling durability test for 10,000 cycles (protocol: 0.6-0.95 V) and a start-stop (carbon corrosion) durability test for 1,000 cycles (protocol: 1 V-1.5 V). Open circuit potential (OCV) and cyclic voltammograms (CVs) were measured periodically during the cycling. EOL iV performance was measured at the end of these durability cycling tests. The accelerated durability protocol used simulates start-up and shut-down of a fuel cell stack as used in a motor vehicle without the application of any operational controls that may mitigate losses. During start up, if the fuel cell stack has been shut down long, the anode and the cathode are filled with ambient air and pinned to air-air potential. Turning on the hydrogen flow causes a hydrogen-air front to move through the anode chamber causing the highest potential of 1.5 V. Thus, in the absence of any mitigating procedure, the cell potential cycles from about 1 V to 1.5 V. During this excursion, the carbon in the cathode corrodes and results in degradation of the catalyst layer.

The recovery process was carried out after the initial 1,000 start-stop durability protocol cycles. During this recovery process, 0.3 to 0.5 A/cm^2 current was drawn from the fuel cell for 16 hours in two steps while supplying fully humidified hydrogen and oxygen at 80° C. under ambient pressure. The reason for using oxygen instead of air for recovery conditioning is that fuel cell could not be operated at high enough steady state current density (~0.5 A/cm^2) using air due to the catalyst degradation during start-stop cycling. OCV, iV performance and CVs were measured after each recovery step. Based on the results for this recovery process, an additional 600 start-stop cycles were carried out in two steps of 300 cycles and similar recovery steps were carried out at the end of these additional potential cycling steps. OCV, iV performance and CVs were measured after these additional potential cycling steps and after the recovery steps to monitor any recovery in iV performance.

With regard to the BOL evaluation of the MEA, FIG. **6**A shows BOL iV performance measured at one bar pressure with and without iR correction data. iR correction for non-PGM cathode catalyst MEA becomes important due to very high amount of ionomer in the catalyst layer and the catalyst layer thickness which result in higher high frequency resistance values. High OCV of ~0.97 V was observed for this catalyst under fully humidified H_2/O_2 0.42/0.84 nlpm at 1 bar_g. Current densities around 750 mA/cm^2 at 0.6 $V_{iR\text{-}free}$/RHE were obtained in comparison with 50-700 mA/cm^2 reported for similar MNC catalysts. Due to the high resistance, iR corrected data shows a significant improvement in iV performance. Volumetric activity or volumetric current density is shown in FIG. **6**B and is calculated at 0.8 $V_{iR\text{-}free}$ voltage without any extrapolation of data in kinetic region and assuming an effective carbon density of 0.4 g/cm^3. Volumetric current density of 31 A/cm^3 was obtained for this melamine based catalyst MEA with a back-pressure of 1 bar.

FIG. **7**A is an SEM image of a metal-nitrogen-carbon catalyst based GDE of its surface morphology at 200×. FIG. **7**B shows an SEM cryofractured cross-sectional view of the metal-nitrogen-carbon catalyst based GDE at 100×. The catalyst layer thickness of ~139 μm was observed compared to a typical thickness of ~10 μm for a platinum based catalyst layer. A thick catalyst layer is a result of the higher catalyst loading requirements for these non-PGM catalysts and higher ionomer contents.

FIG. **8**A shows the effect of load cycling only on iV performance (H_2/O_2 fully humidified at 80° C. and 100 kPa_g). No significant change in iV performance was observed after standard load cycling (BoL vs. EoL) for 10,000 cycles. This shows very positive durability results for non-PGM catalysts under this accelerated standard load test. This high durability can also been demonstrated with no observable change in a double layer capacitance (C_{dl}) or OCV (H_2/O_2 0.5 nlpm for both anode and cathode under atmospheric pressure) values as shown in FIG. **8**B.

FIG. **9**A shows the effect of start-stop cycling and the recovery processes on iV performance (H_2/O_2 fully humidified at 80° C. and 100 kPa_g). A significant drop in iV performance was observed after standard start-stop cycling (BoL vs. EoL) for 1,000 cycles due to the formation of surface oxides (oxygen containing groups such as carboxyl, carbonyl, phenol, carbonyl etc.) and carbon loss. These surface oxides typically make the carbon support more hydrophilic thereby retaining more water in the catalyst layer during fuel cell operation which introduces significant mass transport losses. A passive oxide layer on catalyst surface is also believed to negatively affect the activity of the non-PGM catalyst. Surface oxide formations due to the potential cycling

also resulted in an increased C_{dl} and decreased OCV values (H_2/O_2 0.5 nlpm for both anode and cathode under atmospheric pressure) as shown in FIG. **9**B.

However, an increase or "recovery" in the performance was observed after both recovery steps (After 1^{st} Recovery & After 2^{nd} Recovery) as shown in FIGS. **9**A and **9**B. After the first recovery cycle, significant improvement in iV performance was observed and after the second recovery cycle, iV performance was very close to BOL performance as can be seen in FIG. **9**A. During this recovery process, the created surface oxides on the catalyst surface are removed. The mechanism for surface oxide removal is some combination of the complete oxidization of the surface oxide to carbon dioxide and the reduction back to the original catalyst structure or a modified version of the structure. This recovery in performance can also be observed with an increase of OCV after the recovery steps and a lowering of C_{dl} as shown in FIG. **9**B. Increase in C_{dl} with start-stop cycling can be attributed to formation of the surface oxides, and drop in C_{dl} values after recovery steps indicates the removal of these surface oxides.

During this recovery process, the catalyst may lose some of the carbon support; however even with some carbon loss, this non-PGM catalyst maintains enough carbon to provide adequate electrochemical activity and electronic conductivity. It should be pointed out that the role of the carbon support for non-PGM catalysts is not only for the support/electronic conduction but also as the key player in the electrochemical reaction pathway. Therefore, if enough durability cycles are performed, recovery will no longer be possible.

After performing standard start-stop cycling protocol (up to 1,000 potential cycling), an additional 600 cycles were performed in 300 cycle increments to verify the further recovery of the tested MEA. FIG. **10** shows the effect of the start-stop cycling and the recovery process on the cell potential at 1 A/cm^2. As shown in FIG. **10**, after completion of accumulated 1,300 cycles, the iV performance of MEA dropped significantly and could not sustain 1 A/cm^2. However, as previously seen, MEA performance was able to recover nearly completely after a recovery process performed for sixteen hours.

An additional 300 start-stop cycles were performed and iV performance was measured after the total 1600 cycles. As expected, a significant drop in iV performance was observed. Again the recovery process was carried out to verify any recovery in iV performance. However, after 1600 start-stop cycles, the MEA may have reached the "not recoverable point" and significant recovery was not observed. This is the point where there might not be enough active carbon left in order to be an effective ORR catalyst.

The catalyst recovery processes disclosed herein can be performed on a fuel cell stack in a vehicle without removing or disassembling the fuel cell stack. A vehicle built to be powered by a fuel cell will have the necessary equipment to run the recovery process on an as needed basis. Thus, upon detection of a degraded state or end of life, the vehicle can undergo the recovery process to recover the performance of the fuel cell to at or near beginning of life performance. The system for catalyst recovery of a fuel cell can be installed at a vehicle owner's residence. Alternatively, the owner could approach a dealer or mechanic after being informed of the degraded state or end of life, to have the recovery process performed at the dealer or mechanic's facility, much like one would currently do for an oil change of an internal combustion engine vehicle.

Referring to FIGS. **11-13**, in one system for recovering catalyst performance of a fuel cell stack **310** comprising one or more fuel cells in a vehicle **300** disclosed herein, the system comprises a sensor **312** for detecting EOL of the fuel cell. A notification device **314** notifies a user when the sensor detects EOL of the fuel cell. Means for drawing a steady-state load **316** from the fuel cell stack **310** is used to operate the fuel cell stack **310** until the catalyst performance is recovered.

Also disclosed herein are methods of recovering catalyst performance of a fuel cell in a vehicle. Referring to FIG. **14**, one such method comprises detecting a performance parameter of a fuel cell S**10**, notifying a user of the vehicle when the performance parameter is at or near end of life of the fuel cell S**20** and drawing a steady-state load from the fuel cell until the catalyst performance is recovered S**30**.

The sensor **312** can be located anywhere in the vehicle **300** where it can detect the necessary parameters that will indicate EOL. As defined herein, EOL can be measured with many different parameters, including current, voltage, hours of operation, amount of miles driven, and the like. The sensor **312** can be of any type known to those skilled in the art that is configured to detect the EOL parameters.

The sensor **312** can operate to continuously monitor the EOL parameter while the vehicle **300** is in operation. A controller **318** can be included in the vehicle **300** and can collect the data detected by the sensor **312**. Alternatively, an existing controller or computer in the vehicle can collect the sensor data. The controller **318** can be programmed with one or more predetermined EOL parameter values such that when the sensor **312** detects that the EOL parameter has reached the predetermined value, a notification device **314** notifies the user that the fuel cell stack **310** has reached EOL. As a non-limiting example, if the EOL is defined by a predetermined number of hours of operation, the controller **318** is programmed such that when the sensor **312** detects the predetermined number of hours of operation, the notification device **314** notifies a user of the vehicle **300** that the fuel cell stack **310** has reached EOL and the recovery process should be performed.

The notification device **314** can be located in the vehicle passenger compartment, for example, on the dash board or instrument panel. The notification device **314** may also be on a key fob. The notification device **314** can be a visual indicator such as a light that turns on when EOL is reached or a light that changes color when EOL is reached. The visual indicator **314** can be instructions to run the recovery system. The notification device **314** may also or alternatively be an audio indicator. As a non-limiting example, an alarm such as a beep can sound when EOL if reached and can resound whenever the vehicle is started after EOL is reached. It is also contemplated that the notification device **314** can send a visual notification to an email address or send a text to the user providing instructions to run the recovery system.

The recovery process requires that the fuel cell stack **310** be placed under a steady-state load **316** for a period of time. The recovery system can be provided at a user's residence or can be accessible to a user at a dealer or mechanic's shop for example. The fuel cell stack **310** does not need to be removed from the vehicle **300**. The fuel cell recovery process is done in situ and does not require a high level of mechanical skill. The means for drawing the steady-state load **316** that may be provided at a user's residence can include one or more internal load drawing accessories of the vehicle **300** as indicated in FIG. **11**. Internal load drawing accessories include, for example, vehicle lights, the HVAC system, and other on-board vehicle components. In this way, the recovery process is internal to the vehicle **300** as the process utilizes the fuel gas that is provided in the vehicle's fuel gas tank **320**.

The means for drawing the steady-state load **316** can include hooking the fuel cell stack **310** up to a residential

power grid, such as envisioned for electric vehicles. The fuel cell stack **310** will operate at steady-state using the on-board fuel gas in the fuel gas tank **320** and the power generated would be supplied to the power grid as opposed to operating the vehicle. Another means for drawing the steady-state load **316** can be an external load generator **322** as shown in FIG. **13**, or a load box, that can be attached to the fuel cell stack **310**. A load box **322** may be purchased and installed at a residence or may be used by a technician at a dealer or mechanic's shop. Another example of means for drawing the steady-state load **316** is a dynamometer **324**, as shown in FIG. **12**, a device typically found at dealers and mechanics. The vehicle **300** would be set up on the dynamometer **324** to operate at a steady pace for the required period of time. As mentioned herein, a steady-state load of about 0.3 to 0.5 A/cm^2 is recommended. The examples are not meant to be limiting. Other load generators known to those skilled in the art can be used.

It is contemplated that the vehicle's fuel gas tank **320** is sufficiently sized to provide the fuel gas required during the recovery process. However, an external fuel tank **330** can be provided to increase capacity or to be used in place of the on-board fuel tank **320**. For example, if a vehicle **300** is taken into the dealer or a shop to have the recovery process completed with the dealer's or shop's system, it would eliminate the need to use the vehicle owner's fuel gas and enable accurate measuring of fuel gas usage during the process for quality and cost purposes. The external fuel gas supply **330** can be coupled to the on-board fuel tank **320** to continually supply the fuel cell via the on-board tank **320**, as shown by line **332**, or fuel gas can be supplied directly to the fuel cell stack **310** directly from the external fuel gas supply **330** through a bypass valve **334** that can be added to the existing power generation system of the vehicle **300**, as shown with line **336**.

The means for drawing a steady-state load **316** can be operated for a predetermined period of time. A timer can be used to alert the user or technician that the predetermined time period has elapsed. Alternatively, the timer can be configured to automatically stop the means for drawing a steady-state load **316** and end the recovery process when the predetermined time period has elapsed.

The sensor **312** that detects one or more EOL parameters can also be configured to detect a recovery state of the fuel cell stack **310** while the recovery process is undergoing. Alternatively, a second sensor can be incorporated into the system to detect the recovery state of the fuel cell stack **310**. In either case, the sensor **312** can be configured to stop the means for drawing the steady-state load **316** when the recovery state is detected and/or indicate to the user or technician that the recovery state has been reached. The recovery state can be defined by a predetermined amount of time of operation of the means for drawing the steady-state load, an output voltage of the fuel cell and/or a current of the fuel cell. The recovery state is defined as at or near BOL of the fuel cells as described above.

One or more parameters of the fuel cell stack **310** can be monitored during the recovery process to determine the recovery state, and those parameters can be saved by the controller **318**. It is contemplated that the data can be downloaded for use by the owner of the vehicle or the technician to track the progress of the recovery process to ensure the quality of the recovery.

The exhaust from the fuel cell stack **310** can be monitored during the recovery process to test for other contaminants or to determine how much carbon is being removed during the process. As a non-limiting example, a carbon dioxide detector can be placed on the exhaust of the fuel cell to monitor carbon dioxide exhausted from the fuel cell stack **310** during the recovery process. From the carbon dioxide data, the amount of carbon removed from the catalyst can be calculated. This carbon information can assist in determining the number of recovery cycles that can be performed on the fuel cell stack **310** until the catalyst is unable to be recovered properly. As another non-limiting example, a hydrogen sulfide monitor can be used to monitor the amount of contamination of the fuel cell catalyst and the amount of removal of the contamination. As an additional non-limiting example, an oxide monitor can be used to monitor the amount of oxides (oxygen containing groups of carboxyl, carbonyl, phenol, carbonyl, etc.) being exhausted.

While the invention has been described in connection with what is presently considered to be the most practical and preferred embodiment, it is to be understood that the invention is not to be limited to the disclosed embodiments but, on the contrary, is intended to cover various modifications and equivalent arrangements included within the spirit and scope of the appended claims, which scope is to be accorded the broadest interpretation so as to encompass all such modifications and equivalent structures as is permitted under the law.

What is claimed is:

1. A catalyst recovery process for a fuel cell having a membrane electrode assembly comprising:

detecting a predetermined end of life state of the fuel cell during normal operation of the fuel cell, the normal operation being while the fuel cell is providing a variable load to a device in response to varying power needs of the device as operated; and

in response to detecting the predetermined end of life state, operating a recovery device to perform a first recovery cycle on the fuel cell by:

switching from the variable load to a steady state load, the steady state load achieved by:

supplying fuel gas to an anode of the fuel cell at a steady state and an oxidant to a cathode of the fuel cell at a steady state; and

concurrently drawing a steady current from the fuel cell;

detecting a completion of the first recovery cycle, wherein the first recovery cycle is determined to be complete when the fuel cell is detected to reach a first predetermined recovered performance level.

2. The catalyst recovery process of claim **1**, wherein the first predetermined recovered performance level is a performance level of the fuel cell at or near beginning of life.

3. The catalyst recovery process of claim **1**, wherein the catalyst is a precious metal group catalyst.

4. The catalyst recovery process of claim **1**, wherein the steady current drawn during the first recovery cycle is between about 0.3 to 0.5 A/cm^2.

5. The catalyst recovery process of claim **1**, wherein supplying the fuel gas and oxidant comprises supplying fully humidified fuel gas and an oxidant at between about 70° C. and 90° C.

6. The catalyst recovery process of claim **1**, wherein the oxidant is oxygen and the fuel gas is hydrogen.

7. The catalyst recovery process of claim **1**, wherein the oxidant is air and the fuel gas is hydrogen.

8. The catalyst recovery process of claim **1**, wherein the first predetermined recovered performance level is defined by one or both of an output voltage approximate a beginning of life output voltage of the fuel cell and a current draw approximate a beginning of life current draw of the fuel cell.

9. The catalyst recovery process of claim **1** further comprising:

operating the fuel cell subsequent to the first recovery cycle in the normal operation, providing the variable load to the device in response to the varying power needs of the device;

detecting for a second time a predetermined end of life state of the fuel cell during normal operation of the fuel cell; and

operating the recovery device to perform a second recovery cycle on the fuel cell comprising:

switching from the variable load to the steady state load;

supplying the fuel gas to the anode of the fuel cell at a steady state and the oxidant to the cathode of the fuel cell at a steady state; and

concurrently drawing the steady current from the fuel cell; and

detecting the completion of the second recovery cycle, wherein the second recovery cycle is determined to be complete when the fuel cell is detected to reach a second predetermined recovered performance level.

10. The catalyst recovery process of claim **1**, wherein the first recovery cycle removes surface oxides from carbon in the catalyst.

11. The catalyst recovery process of claim **10**, wherein the surface oxides are removed by oxidation of the surface oxide to carbon dioxide.

12. The catalyst recovery process of claim **10**, wherein the surface oxides are removed by reducing the surface oxides to reproduce an original catalyst structure.

13. The catalyst recovery process of claim **1**, wherein the fuel cell is one of a plurality of fuel cells in a fuel cell stack.

14. The catalyst recovery process of claim **13**, wherein the fuel cell stack is located in a vehicle.

15. The catalyst recovery process of claim **1**, wherein the non-precious metal group catalyst is a metal-nitrogen-carbon type catalyst.

16. The catalyst recovery process of claim **1**, wherein a number of recovery cycles that the fuel cell undergoes is limited by loss of carbon from the catalyst.

17. The catalyst recovery process of claim **1**, wherein the fuel cell is detected to reach the predetermined recovered performance level when a predetermined time period has elapsed.

18. The catalyst recovery process of claim **9**, wherein the second predetermined recovered performance level is inferior to the first predetermined recovered performance level.

19. The catalyst recovery process of claim **17**, wherein the catalyst is a non-precious metal group catalyst and the predetermined time period of the first recovery cycle is about fifteen to about twenty hours.

20. The catalyst recovery process of claim **17**, wherein the predetermined time period of the first recovery cycle is reduced as a recovery pressure is increased, the recovery pressure being a pressure under which the first recovery cycle is performed.

* * * * *